JACS
JOURNAL OF THE AMERICAN CHEMICAL SOCIETY
pubs.acs.org/JACS
Article

Invoking Side-Chain Functionality for the Mediation of Regioselectivity during Ring-Opening Polymerization of Glucose Carbonates

Yue Song, Xin Yang, Yidan Shen, Mei Dong, Yen-Nan Lin, Michael B. Hall, and Karen L. Wooley*

Cite This: J. Am. Chem. Soc. 2020, 142, 16974−16981
Read Online

ABSTRACT: The extent of participation of side-chain functionalities during the 1,5,7-triazabicyclo[5.4.0]dec-5-ene (TBD) organobase-catalyzed ring-opening polymerizations (ROP) of six-membered cyclic D-glucose-based carbonates was found to result in significantly different regiochemical outcomes. High regioselectivity was observed for naturally derived poly(4,6-D-glucose carbonate)s (PGCs) containing carbonate side chain substituents in the 2- and 3-positions, whereas regioirregularity was found for analogous PGCs with ether side-chain substituents. The backbone connectivities and structural details of these PGCs were examined through a combination of comprehensive 1D and 2D NMR studies on unimers and dimers, verifying the ring-opening preferences and indicating the contribution of side-chain functionalities in regioselective ROP processes. A molecular understanding of the curious role of side-chain functionalities was demonstrated via density functional theory calculations, revealing stabilization effects of intermolecular hydrogen bonding between the side-chain functionalities and TBD in the transition states. Overall, this work provides fundamental insights into the organocatalytic ROP of these specific six-membered asymmetric cyclic glucose carbonates. More importantly, these findings serve as a foundation for future design strategies that incorporate adjacent functionalities within monomers to act as directing groups and impart molecular interactions that define regiochemical ring-opening.

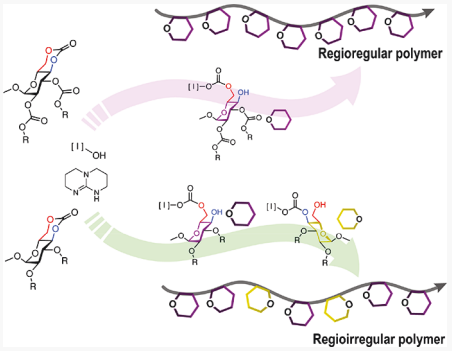

INTRODUCTION

Renewable sugar-based polymers have gained significant attention from chemists and from the broader community, due to their sustainability, structural diversity, potential for degradability, and as alternatives to petrochemicals for commercial applications.[1−3] There have been numerous studies on the development of sugar-based polymers over the past decades, which have often been devoted to the exploration of diversified monomer structures, the incorporation of functionality, the expansion of polymerization methods, and the utilization in various practical applications.[4−9] Among others, glucose is of great interest, owing to its natural abundancy and high degree of functionality for tailoring of physicochemical and mechanical properties. A primary strategy for the construction of well-defined glucose-based polycarbonates has involved controlled ROPs.[10] The guanidine organocatalyst, TBD, has been applied widely for the ROP for a variety of cyclic monomers in the presence of alcohol or amine initiators, while exerting high reactivity and excellent control of polymer molar mass and dispersity.[11−19] More recently, regioselectivity has been observed using TBD during the ring-opening of cyclic carbonates and sugar-based fused-cyclic monomers.[20,21] Despite the importance of regiochemistry in directing synthesis, regulating properties, and thereby affecting polymer performance and applications, studies have seldom focused on revealing the regiochemical structures of the complex glucose-based polymers.

Several studies have probed the regiochemistry during ring-opening reactions of cyclic molecules. Kleij and co-workers achieved the regioselective ring-opening aminolysis of substituted five-membered cyclic carbonates by using TBD as the catalyst.[21] Uryu and co-workers studied the polymerization of 3,5-anhydro-1,2-*O*-isopropylidene-α-D-xylofuranose in which a regioregular [3→5]-2,3-*O*-isopropylidene-α-D-xylofuranan polyether was afforded under various polymerization conditions with a number of Lewis acids, anionic and coordination catalysts.[22] More recently, Buchard and co-workers reported the ring-opening of D-mannose-based 4,6- cyclic carbonate to proceed in a regioselective tail-to-head (T−H) direction, as was confirmed through a joint experimental and computational approach.[20] Aside from a few special cases of regioselective ring-opening reactions, the formation of regioirregular polymers is quite common. For instance, Gross and co-workers reported a

Received: May 22, 2020
Published: September 23, 2020

https://dx.doi.org/10.1021/jacs.0c05610
J. Am. Chem. Soc. 2020, 142, 16974−16981

Scheme 1. ROP of Glucose Carbonate Monomers with Carbonate vs Ether Side Chains, Selectively, Yielding Regioregular and Regioirregular/Regiorandom Polymers, Respectively

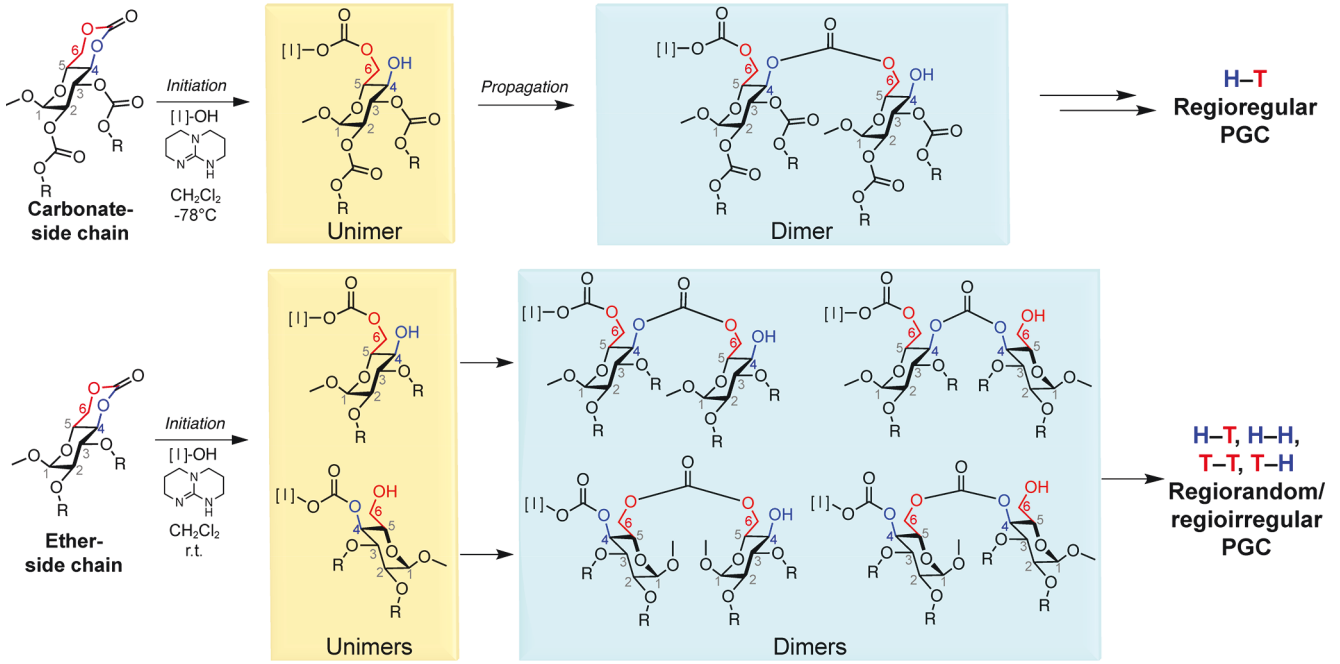

polycarbonate having head-to-head (H−H), head-to-tail (H−T), and tail-to-tail (T−T) backbone linkages in a statistical 1:2:1 ratio from the ROP of a D-xylofuranose-based six-membered cyclic carbonate catalyzed by yttrium(III) tris(isopropoxide).[23]

Within the past decade, we have experimentally observed inconsistencies in the regioregularity/regioirregularity of PGCs derived from the ROP of 4,6- six-membered cyclic carbonate monomers.[24−26] Regioirregular PGCs were observed having statistical H−H, H−T, and T−T repeat unit connectivities from methoxy-protected glucose carbonate monomers,[24] whereas highly regioregular polymers were identified from glucose carbonates with ethyl- and propargyl-carbonate side chains (Scheme 1).[25] In Mikami et al.,[24] we reported the regiorandom nature of methoxy-protected glucose-derived polycarbonates from TBD-catalyzed ROP of a six-membered 4,6-cyclic asymmetric carbonate, as indicated by multiple resonance frequencies attributed to the H−H, H−T, and T−T species in ^{13}C NMR spectra and confirmed by tandem MS analyses using electron transfer dissociation (ETD). In contrast, later works[25,26] indicated the preparation of regioregular PGCs with different alkyl-carbonate protecting groups on the 2- and 3-positions of the glucose carbonate, and the regioregularity persisted regardless of the side chain structures. Understanding these differential regiochemistries during the ROP of D-glucose-based cyclic carbonate monomers having ether vs carbonate side chain functionalities, presented an exciting challenge. More importantly, understanding the regioselectivity and exploring the mechanistic origins are of vital importance for organic-catalytic polymerizations, which would allow for control over polymer chain connectivity and resulting polymer materials properties broadly.

To explore the origin that dictated the regiochemistry and achieve a deep understanding of the TBD-catalyzed ROP process, therefore, herein we report results from investigations during the early stages of polymerization through structural characterization of glucose carbonate unimers and dimers with carbonate or ether side-chain functionalities. Building upon our previous report of the synthesis and isolation of discrete oligomers,[26] full characterization of these compounds was conducted to reveal the detailed structures. Density functional theory (DFT) calculations were also applied to probe the origin of the regioselectivity.

RESULTS AND DISCUSSION

Structures of Discrete Unimers and Dimers with Carbonate Side Chains. Recently, we have investigated the ROP of a broad range of D-glucose carbonate monomers with varied alkyloxycarbonyl side chains; high regioselectivity persisted regardless of the length and branch/bulkiness of the side chain.[25,26] The polymer regioregularity was evidenced by only one sharp peak corresponding to the polymer backbone carbonate C═O resonating at 153.6−153.9 ppm in the ^{13}C NMR spectra of the PGCs. In accordance with the ^{13}C NMR analysis, well-defined splitting patterns for the glucose monomer repeat unit protons of the side chain carbonate-protected PGCs in their ^{1}H NMR spectra contrasted with typical broad peaks for regioirregular polymers, as was observed for side chain ether-protected PGCs. To agree with both the ^{13}C and ^{1}H NMR observations, possible regioisomeric forms of highly regioregular PGC can be either 4-to-6 (H−T) or 6-to-4 (T−H) linkages. Either linkage would lead to regioregularity of the resulting polymers, but were indiscernible from the polymer 1D NMR spectra. However, further structural elucidation of the polymers directly, including homonuclear and heteronuclear 2D NMR techniques, was impeded by the structural and resulting spectroscopic complexities. To reveal the regioselectivity during initiation and propagation steps, the structures of unimers and dimers were examined. Therefore, TBD-catalyzed ring-opening reactions of D-glucose-based cyclic carbonates were conducted in CH_2Cl_2 at −78 °C in the presence of 0.3−0.5 equivalences of 4-methylbenzyl alcohol (4-MeBnOH) to limit chain growth. Oligomeric samples **A1**, **A2** (derived from methyl-2,3-*O*-2-

https://dx.doi.org/10.1021/jacs.0c05610
J. Am. Chem. Soc. 2020, 142, 16974−16981

ethylhexyloxycarbonyl-4,6-*O*-carbonyl-*α*-D-glucopyranoside [GC(EHC^2)]), **B1** and **B2** (derived from methyl-2,3-*O*-neopentyloxycarbonyl-4,6-*O*-carbonyl-*α*-D-glucopyranoside [GC(neoPC^2)]) (Figure 1) were prepared, followed by

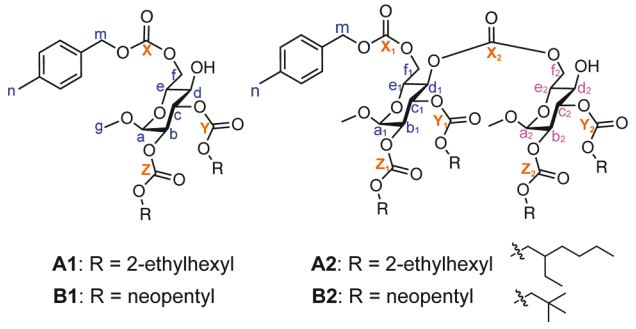

Figure 1. Unimer and dimer structures of 2-ethylhexyl- (**A1** and **A2**, respectively) and neopentyl- (**B1** and **B2**, respectively) D-glucose carbonates that were synthesized, isolated by SEC, and determined to have the particular regiochemistries shown here, from NMR investigations of the ring-opening directions of monomers with carbonate-based side chain protecting groups.

fractionation using preparative size exclusion chromatography (SEC) to isolate sufficient quantities of unimeric and dimeric structures for detailed NMR analyses.

Homonuclear correlation spectroscopy (COSY; Figures 2a and S1), ^{1}H−^{13}C heteronuclear single quantum correlation (HSQC; Figure S2), and ^{1}H−^{13}C heteronuclear multiple-bond correlation (HMBC; Figure 2b) 2D-NMR analyses were performed to examine the structural details, thereby providing regioselective preferences of ring-opening reactions during initiation and propagation. First, each proton of **A1** was assigned by combining the results from ^{1}H NMR, COSY, and HSQC. The unimer structure was found to have the C4 position linked to a free hydroxyl group, as indicated by the COSY spectrum showing a cross peak at (3.69, 3.10 ppm), designated to the coupling of the O***H*** and C-$\boldsymbol{H}_d$ protons, while no cross peak between $\boldsymbol{H}_f$ and O***H*** was observed. Meanwhile, by HMBC, the presence of a critical $^3J_{CH}$ coupling between the backbone carbonyl carbon and the protons on C6 (C$\boldsymbol{H}_f$), $^3J_{X\text{-}f}$ at 155.45, 4.43 ppm, suggested the C−O6 bond was retained (Figure 2b). The absence of J_{CH} between the $\boldsymbol{H}_d$ proton with any carbonyl carbon in the HSQC spectrum further verified the cleavage of the C−O4 bond. The absence of correlation between the alcohol proton (3.06 ppm) and any carbon in HSQC (Figure S2) gave the same conclusion. These combined results suggested that the initiation reaction of the ring-opening polymerization with 4-MeBnOH was favorable with cleavage occurring at the C−O4 position, yielding a secondary alcohol on the C4 position as the active chain-end for the following propagation process.

To study whether the same regioselectivity was maintained in the following propagation step of ROP from the unimer, COSY (Figures 2c, S3), ^{1}H−^{13}C HSQC (Figure S5), and ^{1}H−^{13}C HMBC spectra (Figure 2d) of the dimer of GC(EHC^2) (**A2**) were acquired. Similarly, two sets of proton resonances in the ^{1}H NMR spectrum that correlated to the first and second repeating

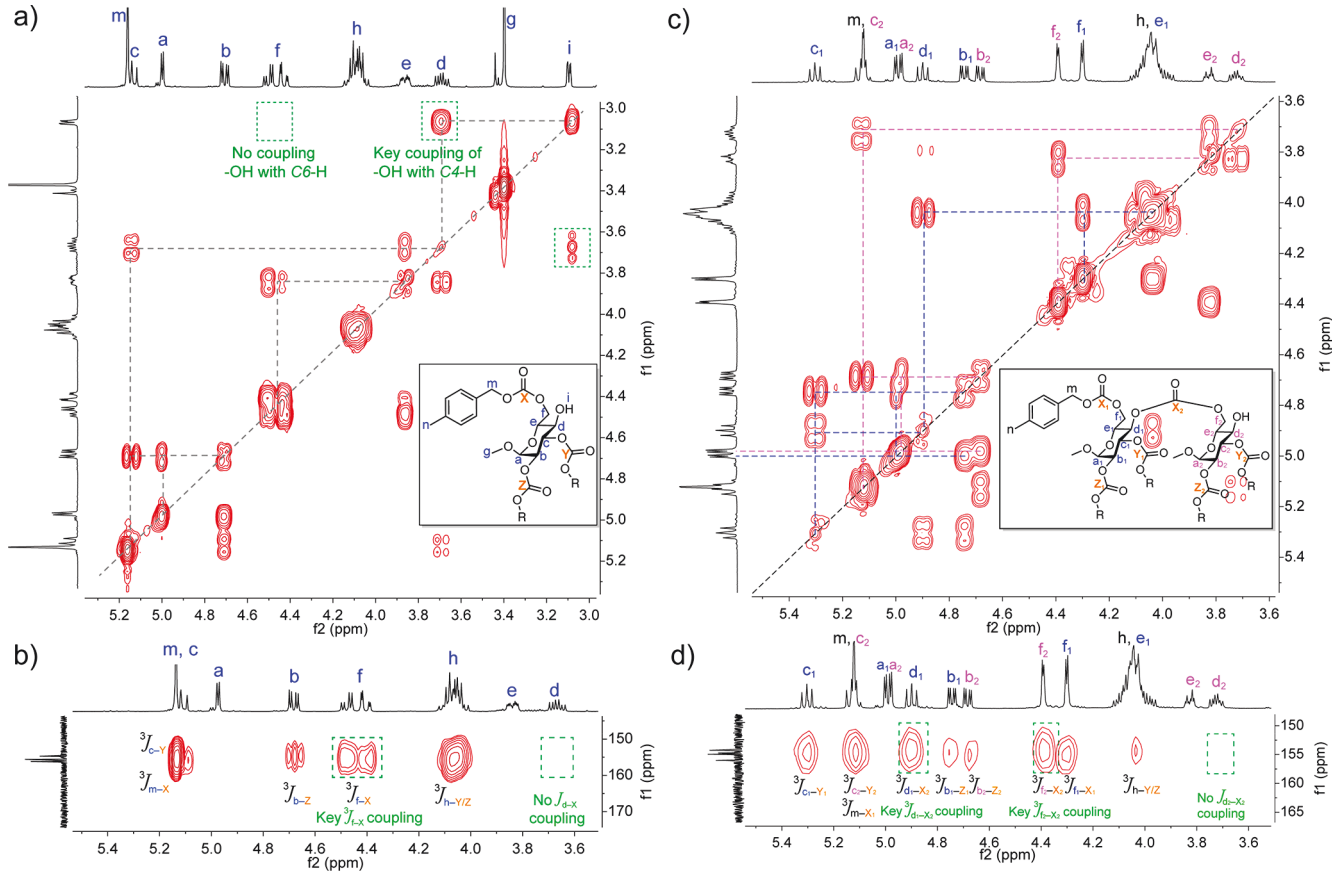

Figure 2. COSY and ^{1}H−^{13}C HMBC spectra (400 MHz for ^{1}H) of GC(EHC^2) unimer and dimer in $CDCl_3$. (a) COSY and (b) ^{1}H−^{13}C HMBC spectra of the unimer; (c) COSY and (d) ^{1}H−^{13}C HMBC of the dimer. The peaks labeled with *h* are attributed to side chain R group.

https://dx.doi.org/10.1021/jacs.0c05610
J. Am. Chem. Soc. 2020, 142, 16974−16981

units of the D-glucose carbonates were assigned before further analysis. From HMBC spectroscopy, the presence of a key $^3J_{CH}$ coupling between the backbone carbonyl carbon of the second repeating unit ($\boldsymbol{C}_{X2}$) and the protons on C6 ($\boldsymbol{H}_{f2}$) at (154.81, 4.39 ppm), together with the absence of the carbonyl carbon with the proton on C4 ($\boldsymbol{H}_{d2}$, 3.72 ppm), revealed the sustained C−O6 linkage and occurrence of C−O4 cleavage during addition of the second repeat unit during the propagation process. Further evidence of this dimer connection was found by comparing the chemical shifts of the protons connected to C4 and C6 in both repeating units. The protons on C6 ($\boldsymbol{H}_{f1}$ and $\boldsymbol{H}_{f2}$) in both repeating units possessed similar downfield chemical shifts at 4.30 and 4.39 ppm, respectively, indicative of their connections to the backbone carbonate groups. In contrast, distinctly different chemical shifts were observed for the C4 protons ($\boldsymbol{H}_{d1}$ and $\boldsymbol{H}_{d2}$) of the two dimer repeat units, revealing their varied chemical environments. The more deshielded resonance of $\boldsymbol{H}_{d1}$ (4.90 ppm) was attributed to the connectivity of C4 in the first repeating unit to a carbonate group. The C4 in the second repeating unit was found to be attached to a free hydroxyl group by comparing the chemical shift of $\boldsymbol{H}_{d2}$ (3.72 ppm) and $\boldsymbol{H}_{d}$ (3.69 ppm) of the unimer. Therefore, both of the unimer and dimer structures exhibited preference in the formation of backbone carbonate linkages at the less sterically hindered primary (6-) position, and leaving the secondary hydroxyl group of the 4-position for subsequent propagation, affording the regioregular 4-to-6 H−T linkages. When the 2-ethylhexyl carbonate-substituted side chains of the monomer were changed to neopentyl carbonate (**B1** and **B2**), the same regiochemistry was preferred, based on analyses of the corresponding unimer and dimer structures (Figures S5−S10). This regioselective ROP process was in agreement with recent reports by Sopeña et al.[21] and Gregory et al.[20] in the synthesis of carbamates and mannose-based polycarbonates, respectively, where the initiator attacked the cyclic carbonate carbonyl during the addition step and selectively cleaved the bond to the more hindered group during the elimination.

Synthesis and Structural Analyses of Regioisomers with Ether Side Chains. To investigate the roles of steric hindrance and/or electronic effects in the findings of side chain carbonate groups mediating regioselective preference of the ring-opening reactions during initiation and propagation of alkyloxycarbonyl protected D-glucose carbonates (vide supra), a parallel study was performed on D-glucose-based carbonate monomers with ethylhexyl and methyl side chain alkyl structures, but having ether-linkages at the 2- and 3- positions. Methyl-2,3-*O*-2-ethylhexyl-4,6-*O*-carbonyl-*α*-D-glucopyranoside, a glucose carbonate containing two ethylhexyl ether side chains [GC(EHE^2)], was synthesized using modified procedures from previous reports (Figure S14),[24] followed by which PGC(EHE^2) (12.3 kDa, $Đ$ = 1.16) was afforded through ROP with 4-MeBnOH and TBD at room temperature in a glovebox (Figure 3). Room temperature was employed for these reactions, initially, to be in agreement with the previous polymerization studies. Unfortunately, attempts at conducting these reactions at −78 °C to be in agreement with the carbonate side chain monomers led to insolubility challenges. In contrast to the ^{13}C NMR and ^{1}H NMR spectra of PGCs with carbonate-side chains, multiple broad peaks in the region of 154.0−155.5 ppm and ill-defined broad resonances in ^{1}H NMR were found for this analogue PGC with ethylhexyl ether-side chains, suggesting the existence of a variety of backbone linkages (H−H, H−T, and T−T) and a regioirregular polymer structure.

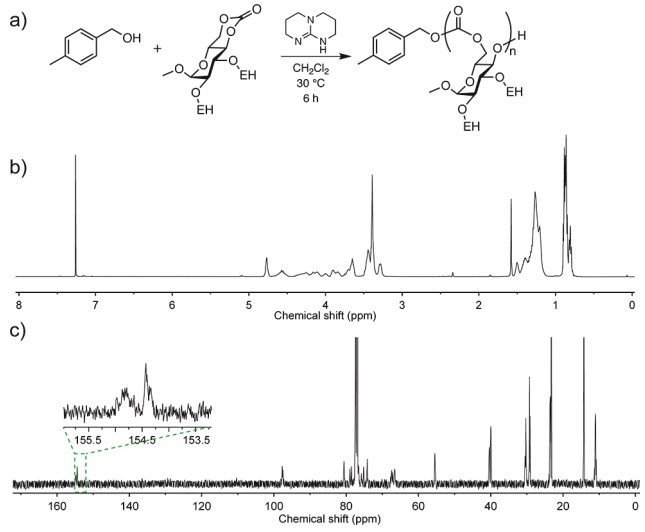

Figure 3. (a) Synthesis of PGC(EHE^2); (b) ^{1}H (500 MHz) and (c) ^{13}C NMR (126 MHz) spectra of the polymer in $CDCl_3$ (inset: zoom in from 156−153 ppm).

Similar oligomer synthesis, isolation and characterization by 1D and 2D NMR analysis methods that had been employed for GC(EHC^2) and GC(neoPC^2) were applied to this GC(EHE^2) to further confirm the regioirregular characteristics, and to quantitatively probe the regioselectivity preference.

In particular, when the unimer of GC(EHE^2) was synthesized and isolated using preparative SEC, it was found to exist as two regioisomers, each of which was further separated using preparative thin-layer chromatography (TLC) and identified using a combination of 1D and 2D NMR spectroscopic characterization. Oligomerization was conducted with 4-MeBnOH and GC(EHE^2) at a molar ratio of 1:1, in the presence of TBD at room temperature in a glovebox. The reaction was allowed to proceed for 1.5 h prior to being quenched by the addition of acetic acid. From this oligomeric mixture, fractionation by preparative SEC allowed for isolation of a mixture of regioisomeric unimers **I** and **II** (Figures 4 and S12). The quantitative ratio of the two regioisomers was determined from the ^{1}H NMR spectrum by comparing the integrations of the signals resonating at 4.82 vs 4.79 ppm and 3.32 vs 3.27 ppm, resulting in a ratio of 1:4 (Figure 4a). These two unimers having the same molar mass were then separated using preparative TLC (Figure S16), where each fraction of the isomeric unimers was identified using high-resolution mass spectrometry (HRMS) and NMR spectroscopy. HMBC spectroscopy provided critical information to structurally distinguish these two isomeric unimers (Figure 4c,d), by differentiating couplings between the carbonyl carbon and either $\boldsymbol{H}_{d}$ or $\boldsymbol{H}_{f}$ proton(s). Isomer **I** presented a $^3J_{CH}$ coupling between the carbonyl signal with the C6 proton ($\boldsymbol{H}_{f}$) resonating at 155.50, 4.40 ppm, supporting the linkage of C−O6. In contrast, a $^3J_{CH}$ coupling of the carbonyl carbon was observed with the proton ($\boldsymbol{H}_{d}$) on C4 resonating at 155.50, 4.70 ppm for **II**, which confirmed the identity of **II** to be the C−O4 isomer. Taken together, these results for the two regioisomeric unimers of GC(EHE^2), **I** and **II**, indicate that the preference between the C−O4 and C−O6 cleavage in the ring-opening initiation step was determined to be 4:1, respectively, again showing a preference for cleavage of the most sterically hindered group from the tetrahedral intermediate.

https://dx.doi.org/10.1021/jacs.0c05610
J. Am. Chem. Soc. 2020, 142, 16974−16981

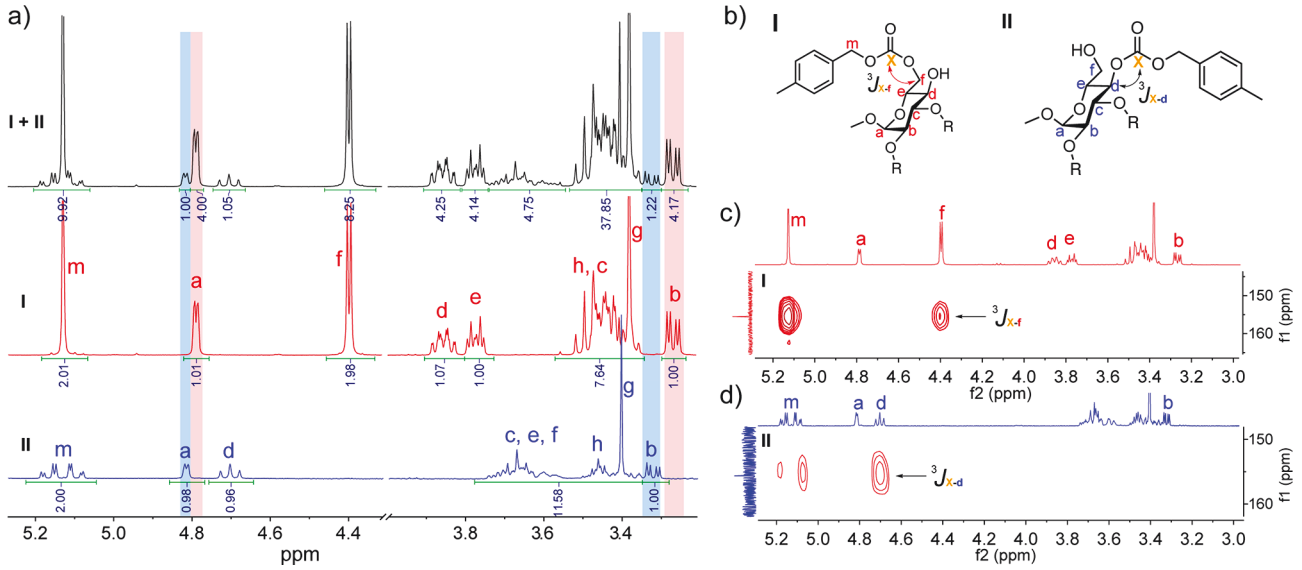

Figure 4. Analysis of the 2-ethylhexyl ether protected unimers of GC(EHE^2). (a) ^{1}H NMR (400 MHz, $CDCl_3$) spectra of a crude mixture of the unimeric isomers (unimers **I** + **II**, black curve), isomer **I** (red curve) and isomer **II** (blue curve). (b) Structures (R = 2-ethylhexyl) and HMBC spectra of (c) isomer **I** and (d) isomer **II** showing cross-peaks of $^3J_{C-H}$ correlations of C-H_f for **I**, and C-H_d for **II**, respectively.

For ether side-chain substituted PGCs, differences in polymer backbone regioirregularity were observed between 2-ethylhexyloxy- and methoxy-substituted PGCs. In study of the ROP of methyl-2,3-*O*-methyl-4,6-*O*-carbonyl-*α*-D-glucopyranoside [GC(OMe)], a higher preference for C−O4 cleavage of ca. 92% regioselectivity was found in the initiation step based on the unimer structure (Figure S22). Surprisingly, this selectivity diminished in the propagation step when a second repeating unit was grown, as demonstrated by four distinct carbonyl signals of ca. 1:1:1:1 ratio, and two sets of signals attributed to aromatic initiator carbons in the ^{13}C NMR spectrum of GC(OMe) dimers (Figure S23). Therefore, the regiorandom feature of PGCs with methoxy-protecting side-chains mainly resulted from the propagation process rather than the initiation step.

Taken together, it was found that both steric and electronic effects contributed to the selectivity during ring-opening processes, allowing for tuning the regiochemical outcome of corresponding polymers through intentional incorporation of different side-chain functionalities to act as directing groups at varying extents. For carbonate side chains, regardless of the spatial size of the alkyl substituents, highly regioselective ROPs occur, indicating possible interactions between the corresponding side chain carbonyl with the reaction center. In these cases, carbonate side chains seem to invoke dominating electronic effects. With ether side chains and the lack of a side chain carbonyl, the situation is more complicated, with steric effects being involved to different degrees for initiation and propagation.

DFT Calculations of the Initiation Step during ROP. Inspired by the work of Buchard and co-workers,[20] we investigated the initiation step during the ROP of glucose carbonate with DFT calculations (see computational details in the SI). In accordance with previous ROP mechanistic studies,[27−30] the initiator and monomer undergo a simultaneous activation of bifunctional TBD through a hydrogen bonding mechanism, followed by TBD migration to activate a C−O bond of the tetrahedral intermediate and afford the propagating alcohol chain end (Figure S26). Four different structural arrangements (paths a−d) of the starting materials were calculated. For paths a and b, the initiator attacked anti to the anomeric methoxy group of the monomer, yielding a primary alcohol chain through C−O6 cleavage (path a), or a secondary alcohol chain via C−O4 cleavage (path b). Similar mechanisms were proposed for path c (C−O6 cleavage) and path d (C−O4 cleavage) when the initiator attacked syn to the anomeric methoxy group. In agreement with experimental results, energy differences were observed at the second transition states (TS2) in Figure S27, with the more stable configurations leading to C−O4 cleavage products, and the less stable ones leading to C−O6 cleavage products. The differences of the Gibbs free energy barriers found between C−O4 cleavage and C−O6 cleavage were at least 2.0 kcal/mol, which were sufficient to make a rate difference over an order of magnitude under the reaction conditions at −78 °C.

Noteworthy, intermolecular hydrogen bonding was found as another critical factor contributing to the regioselectivity. In addition to common N−H···O hydrogen bonding during the reaction, C−H···O hydrogen bonding was also observed for TS2-*b* and TS2-*d* between the TBD and side-chain carbonyl in the 3-positions (Figure 5). This C−H···O interaction has been reported to assist and often control molecular recognition, supramolecular interactions,[31,32] as well as and can play an important role in stabilizing intermolecular complexes.[33,34] During the critical ring-opening C−O4 bond cleavage in TS2-*b* and TS2-*d*, the existence of C7−H7···O7 and C8−H8···O7 hydrogen bonds were demonstrated by the distances of [H···O] = 2.5−3.2 Å and the angles of C−H···O = 100−140°, which may stabilize the TS complexes and facilitate the ring-opening activation. This hydrogen bonding would also bring TBD in the vicinity of 4-position, thus facilitating the N−H activation and allowing for the selective cleavage of the C−O4 bond, a process analogous to remote directing groups in transition metal catalysis and organometallic reagents.[35] In contrast, TBD was far from the side chains when activating C−O6 bonds so that the C−H···O interactions were not present, leading to less stable complexes TS2-*a* and TS2-*c* (Figure 5). Additionally, the transition state geometries of TS2-*b* and TS2-*d* were structurally

https://dx.doi.org/10.1021/jacs.0c05610
J. Am. Chem. Soc. 2020, 142, 16974−16981

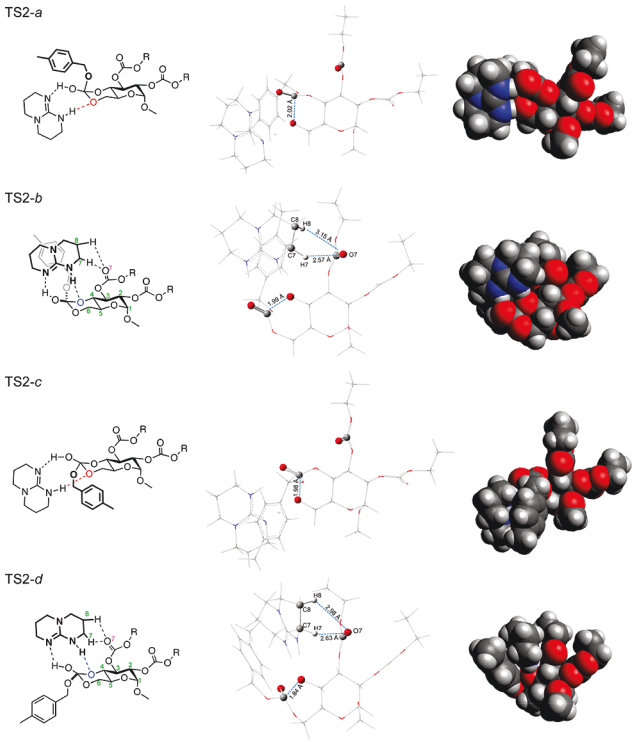

Figure 5. ChemDraw illustrations and optimized geometries of the four structures in TS2, R = ethyl: TS2-*a*: C−O6 cleavage, imaginary frequency f = 304.2i, TS2-*b*: C−O4 cleavage, f = 252.7i, TS2-*c*: C−O6 cleavage, f = 229.9i, and TS2-*d*: C−O4 cleavage, f = 282.6i.

more compact than TS2-*a* and TS2-*c*, which might also assist in stabilizing the transition state.

This hydrogen bonding was not observed in the transition state geometries when we performed DFT calculations on the GC(OMe) monomers (Figure S28). The Gibbs free energies for the two TS2 geometries associated with C−O4 bond cleavage were also higher without the stabilization from hydrogen bonding, illustrating the importance of side chain interaction with TBD in lowering the energy barriers. This hypothesis was also supported by the experimental result of PGC(EHC^2) prepared using a different monofunctional organobase catalyst 1,8-diazabicyclo[5.4.0]undec-7-ene (DBU) at −78 °C, which resulted in regioirregular polymers, as demonstrated by the presentation of multiple carbonyl peaks in the ^{13}C NMR spectrum (Figure S25).

CONCLUSIONS

In summary, we have demonstrated the side-chain-mediated regioselectivity of the ROP of D-glucose carbonate cyclic monomers through syntheses and isolation of discrete unimers and dimers and characterization of their exact structural details during the initial stages of polymerization. From a comprehensive 1D and 2D NMR analyses of the unimers and dimers of D-glucose carbonate **A1**, **A2**, **B1**, and **B2**, in combination with previous observations of distinct peaks in the ^{13}C NMR spectra of relevant polymers, PGCs with carbonate-side chains were concluded to be exclusively 4-to-6 H−T backbone linkages throughout the polymer chains. Further, this analysis approach was extended for quantitative determination of the regioselectivity during the initiation stages of regioirregular PGCs containing ether-substituents. By comparing regioisomeric unimers of glucose carbonates having 2-ethylhexyl ether side chains, a 4:1 ratio between C−O4 vs C−O6 cleavage products was observed, in agreement with the regioirregular property of the polymers. Furthermore, it was found that the ROP of monomers with methyl ether side chains possessed a regioselective initiation step but a nonselective propagation process. Lastly, the regioselectivity of the initiation step was validated by the DFT calculations, revealing the change in product distribution was most likely arising from the structural and energetic difference of the transition states at the C−O cleavage step occurring with distinct spatial arrangements of TBD and the intermolecular interaction of C−H···O hydrogen bonding with the side-chain carbonyl group of the carbonate in the 3-position. A factor that remains a question is the role of temperature; the ROP of monomers containing carbonate side chains was conducted at −78 °C, whereas monomers having ether side chains required higher (ambient) temperature. In additional experiments, motivated by comments of referees during the review of this manuscript, we conducted polymerization of the carbonate monomer GC(EHC^2) at room temperature, and performed ^{13}C NMR analysis on the resulting polymer. It is noticeable from the ^{13}C NMR spectrum (Figure S24) that the carbonyl resonance at 153.9 ppm attributed to the polymer backbone carbonate linkages is broader than those of the side-chain carbonyl peaks, demonstrating that the polymer contained a relatively lower backbone regioregularity compared to the polymer synthesized at −78 °C. This phenomenon is in agreement with the DFT calculation results, that the smallest energy barrier between the two regioisomer transition states is ca. 2.0 kcal/mol at −78 °C, and could be overcome at higher temperature. However, the finding of regioirregularity for the ring opening of the carbonate side chain monomer in the presence of DBU emphasizes the roles that sterics and electronics play. Overall, this work advanced fundamental understandings of the polymerization behavior and polymer regiochemistry of D-glucopyranose-based 4,6-cyclic carbonates. Even more attractive is the use of monomer side-chain groups to intentionally enable catalyst-substrate intermolecular interactions and direct the regiochemical outcome of the polymerization. We anticipate that this exploration of reasons behind the variation of ring-opening preferences in the ROP system will further the development of the next generation of sugar-based polymers.

ASSOCIATED CONTENT

Supporting Information

The Supporting Information is available free of charge at https://pubs.acs.org/doi/10.1021/jacs.0c05610.

Experimental procedures; computational details; additional ^{1}H NMR, COSY, HSQC, HMBC, SEC, and MALDI data (PDF)

Additional molecular structures as discussed in the text (ZIP)

Additional molecular structures as discussed in the text (ZIP)

AUTHOR INFORMATION

Corresponding Author

Karen L. Wooley − *Department of Chemistry, Chemical Engineering, and Department of Materials Science & Engineering, Texas A&M University, College Station, Texas 77842, United States;* orcid.org/0000-0003-4086-384X; Email: wooley@chem.tamu.edu

https://dx.doi.org/10.1021/jacs.0c05610
J. Am. Chem. Soc. 2020, 142, 16974−16981

Authors

Yue Song − *Department of Chemistry, Texas A&M University, College Station, Texas 77842, United States;* orcid.org/0000-0002-7800-5528

Xin Yang − *Department of Chemistry and Laboratory for Molecular Simulation, Texas A&M University, College Station, Texas 77842, United States;* orcid.org/0000-0003-0085-7859

Yidan Shen − *Department of Materials Science & Engineering, Texas A&M University, College Station, Texas 77842, United States*

Mei Dong − *Department of Chemistry, Texas A&M University, College Station, Texas 77842, United States;* orcid.org/0000-0002-9862-0296

Yen-Nan Lin − *Department of Chemistry and College of Medicine, Texas A&M University, College Station, Texas 77842, United States;* orcid.org/0000-0001-7118-7771

Michael B. Hall − *Department of Chemistry and Laboratory for Molecular Simulation, Texas A&M University, College Station, Texas 77842, United States;* orcid.org/0000-0003-3263-3219

Complete contact information is available at: https://pubs.acs.org/10.1021/jacs.0c05610

Notes

The authors declare no competing financial interest.

■ ACKNOWLEDGMENTS

This work is supported by the National Science Foundation (CHE-1610311, CHE-2003771, DMR-1905818, and DMREF-1629094), the Robert A. Welch Foundation through the W. T. Doherty-Welch Chair in Chemistry (A-0001), and the use of the Texas A&M University Laboratory for Synthetic-Biologic Interactions. Work on calculations was supported by the National Science Foundation (CHE-1664866) and the Robert A. Welch Foundation (A-0648). We appreciate contributions from Dr. Yohannes H. Rezenom for obtaining mass spectrometry data, and the Laboratory for Molecular Simulation (https://lms.chem.tamu.edu) and the High-Performance Research Computing Facility (http://hprc.tamu.edu) for providing computing resources useful in conducting the research reported in this article. We also thank Prof. Lei Fang for access to the preparative SEC, with experimental assistance from Ms. Xiaozhou Ji.

■ REFERENCES

(1) Galbis, J. A.; García-Martín, M. d. G.; de Paz, M. V.; Galbis, E. Synthetic Polymers from Sugar-Based Monomers. *Chem. Rev.* **2016**, *116* (3), 1600−1636.

(2) Xie, Y.; Peng, C.; Gao, Y.; Liu, X.; Liu, T.; Joy, A. Mannose-based graft polyesters with tunable binding affinity to concanavalin A. *J. Polym. Sci., Part A: Polym. Chem.* **2017**, *55* (23), 3908−3917.

(3) Xiao, R.; Grinstaff, M. W. Chemical synthesis of polysaccharides and polysaccharide mimetics. *Prog. Polym. Sci.* **2017**, *74*, 78−116.

(4) Piccini, M.; Leak, D. J.; Chuck, C. J.; Buchard, A. Polymers from sugars and unsaturated fatty acids: ADMET polymerisation of monomers derived from D-xylose, D-mannose and castor oil. *Polym. Chem.* **2020**, *11* (15), 2681−2691.

(5) Desport, J. S.; Mantione, D.; Moreno, M.; Sardón, H.; Barandiaran, M. J.; Mecerreyes, D. Synthesis of three different galactose-based methacrylate monomers for the production of sugar-based polymers. *Carbohydr. Res.* **2016**, *432*, 50−54.

(6) López-Vidal, E. M.; Gregory, G. L.; Kociok-Köhn, G.; Buchard, A. Polymers from sugars and CS2: synthesis and ring-opening polymerisation of sulfur-containing monomers derived from 2-deoxy-D-ribose and D-xylose. *Polym. Chem.* **2018**, *9* (13), 1577−1582.

(7) Gregory, G. L.; Lopez-Vidal, E. M.; Buchard, A. Polymers from sugars: cyclic monomer synthesis, ring-opening polymerisation, material properties and applications. *Chem. Commun.* **2017**, *53* (14), 2198−2217.

(8) Xiao, R.; Zeng, J.; Grinstaff, M. W. Biologically Active Branched Polysaccharide Mimetics: Synthesis via Ring-Opening Polymerization of a Maltose-Based β-Lactam. *ACS Macro Lett.* **2018**, *7* (7), 772−777.

(9) Shearouse, W. C.; Lillie, L. M.; Reineke, T. M.; Tolman, W. B. Sustainable Polyesters Derived from Glucose and Castor Oil: Building Block Structure Impacts Properties. *ACS Macro Lett.* **2015**, *4* (3), 284−288.

(10) Shaver, M.; Buchard, A. Ring opening polymerisation. *Eur. Polym. J.* **2020**, *129*, 109600.

(11) Lohmeijer, B. G. G.; Pratt, R. C.; Leibfarth, F.; Logan, J. W.; Long, D. A.; Dove, A. P.; Nederberg, F.; Choi, J.; Wade, C.; Waymouth, R. M.; Hedrick, J. L. Guanidine and Amidine Organocatalysts for Ring-Opening Polymerization of Cyclic Esters. *Macromolecules* **2006**, *39* (25), 8574−8583.

(12) Sanders, D. P.; Fukushima, K.; Coady, D. J.; Nelson, A.; Fujiwara, M.; Yasumoto, M.; Hedrick, J. L. A Simple and Efficient Synthesis of Functionalized Cyclic Carbonate Monomers Using a Versatile Pentafluorophenyl Ester Intermediate. *J. Am. Chem. Soc.* **2010**, *132* (42), 14724−14726.

(13) Tempelaar, S.; Mespouille, L.; Coulembier, O.; Dubois, P.; Dove, A. P. Synthesis and post-polymerisation modifications of aliphatic poly(carbonate)s prepared by ring-opening polymerisation. *Chem. Soc. Rev.* **2013**, *42* (3), 1312−1336.

(14) Iwasaki, Y.; Yamaguchi, E. Synthesis of Well-Defined Thermoresponsive Polyphosphoester Macroinitiators Using Organocatalysts. *Macromolecules* **2010**, *43* (6), 2664−2666.

(15) Li, R.; Elsabahy, M.; Song, Y.; Wang, H.; Su, L.; Letteri, R. A.; Khan, S.; Heo, G. S.; Sun, G.; Liu, Y.; Wooley, K. L. Functional, Degradable Zwitterionic Polyphosphoesters as Biocompatible Coating Materials for Metal Nanostructures. *Langmuir* **2019**, *35* (5), 1503−1512.

(16) Wang, H.; Dong, M.; Khan, S.; Su, L.; Li, R.; Song, Y.; Lin, Y.-N.; Kang, N.; Komatsu, C. H.; Elsabahy, M.; Wooley, K. L. Acid-Triggered Polymer Backbone Degradation and Disassembly to Achieve Release of Camptothecin from Functional Polyphosphoramidate Nanoparticles. *ACS Macro Lett.* **2018**, *7* (7), 783−788.

(17) Song, Y.; Chen, Y.; Su, L.; Li, R.; Letteri, R. A.; Wooley, K. L. Crystallization-driven assembly of fully degradable, natural product-based poly(L-lactide)-*block*-poly(α-D-glucose carbonate)s in aqueous solution. *Polymer* **2017**, *122*, 270−279.

(18) Pati, D.; Feng, X.; Hadjichristidis, N.; Gnanou, Y. Hydrophobic, Hydrophilic, and Amphiphilic Polyglycocarbonates with Linear and Macrocyclic Architectures from Bicyclic Glycocarbonates Derived from CO2 and Glucoside. *Macromolecules* **2017**, *50* (4), 1362−1370.

(19) Moins, S.; Hoyas, S.; Lemaur, V.; Orhan, B.; Delle Chiaie, K.; Lazzaroni, R.; Taton, D.; Dove, A. P.; Coulembier, O. Stereoselective ROP of rac-and meso-Lactides Using Achiral TBD as Catalyst. *Catalysts* **2020**, *10* (6), 620.

(20) Gregory, G. L.; Jenisch, L. M.; Charles, B.; Kociok-Köhn, G.; Buchard, A. Polymers from Sugars and CO2: Synthesis and Polymerization of a D-Mannose-Based Cyclic Carbonate. *Macromolecules* **2016**, *49* (19), 7165−7169.

(21) Sopeña, S.; Laserna, V.; Guo, W.; Martin, E.; Escudero-Adán, E. C.; Kleij, A. W. Regioselective Organocatalytic Formation of Carbamates from Substituted Cyclic Carbonates. *Adv. Synth. Catal.* **2016**, *358* (13), 2172−2178.

(22) Uryu, T.; Koyama, Y.; Matsuzaki, K. Selective ring-opening polymerization of 3,5-anhydro-1,2-O-isopropylidene-α-D-xylofuranose synthesis of [3→5]-D-xylan. *Makromol. Chem.* **1984**, *185* (10), 2099−2107.

(23) Shen, Y. Q.; Chen, X. H.; Gross, R. A. Polycarbonates from sugars: Ring-opening polymerization of 1,2-O-isopropylidene-D-

xylofuranose-3,5-cyclic carbonate (IPXTC). *Macromolecules* **1999**, *32* (8), 2799−2802.
(24) Mikami, K.; Lonnecker, A. T.; Gustafson, T. P.; Zinnel, N. F.; Pai, P. J.; Russell, D. H.; Wooley, K. L. Polycarbonates derived from glucose via an organocatalytic approach. *J. Am. Chem. Soc.* **2013**, *135* (18), 6826−9.
(25) Su, L.; Khan, S.; Fan, J. W.; Lin, Y. N.; Wang, H.; Gustafson, T. P.; Zhang, F. W.; Wooley, K. L. Functional sugar-based polymers and nanostructures comprised of degradable poly(D-glucose carbonate)s. *Polym. Chem.* **2017**, *8* (10), 1699−1707.
(26) Song, Y.; Ji, X.; Dong, M.; Li, R.; Lin, Y. N.; Wang, H.; Wooley, K. L. Advancing the Development of Highly-Functionalizable Glucose-Based Polycarbonates by Tuning of the Glass Transition Temperature. *J. Am. Chem. Soc.* **2018**, *140* (47), 16053−16057.
(27) Dove, A. P. Organic Catalysis for Ring-Opening Polymerization. *ACS Macro Lett.* **2012**, *1* (12), 1409−1412.
(28) Simon, L.; Goodman, J. M. The mechanism of TBD-catalyzed ring-opening polymerization of cyclic esters. *J. Org. Chem.* **2007**, *72* (25), 9656−62.
(29) Chuma, A.; Horn, H. W.; Swope, W. C.; Pratt, R. C.; Zhang, L.; Lohmeijer, B. G. G.; Wade, C. G.; Waymouth, R. M.; Hedrick, J. L.; Rice, J. E. The Reaction Mechanism for the Organocatalytic Ring-Opening Polymerization of l-Lactide Using a Guanidine-Based Catalyst: Hydrogen-Bonded or Covalently Bound? *J. Am. Chem. Soc.* **2008**, *130* (21), 6749−6754.
(30) Tsao, Y.-Y. T.; Smith, T. H.; Wooley, K. L. Regioisomeric Preference in Ring-Opening Polymerization of 3′,5′-Cyclic Phosphoesters of Functional Thymidine DNA Analogues. *ACS Macro Lett.* **2018**, *7* (2), 153−158.
(31) Gu, Y.; Kar, T.; Scheiner, S. Fundamental Properties of the CH···O Interaction: Is It a True Hydrogen Bond? *J. Am. Chem. Soc.* **1999**, *121* (40), 9411−9422.
(32) Raymo, F. M.; Bartberger, M. D.; Houk, K. N.; Stoddart, J. F. The Magnitude of [C−H···O] Hydrogen Bonding in Molecular and Supramolecular Assemblies. *J. Am. Chem. Soc.* **2001**, *123* (38), 9264−9267.
(33) Vargas, R.; Garza, J.; Friesner, R. A.; Stern, H.; Hay, B. P.; Dixon, D. A. Strength of the NH···OC and CH···OC Bonds in Formamide and N-Methylacetamide Dimers. *J. Phys. Chem. A* **2001**, *105* (20), 4963−4968.
(34) Vargas, R.; Garza, J.; Dixon, D. A.; Hay, B. P. How Strong Is the Cα−H···OC Hydrogen Bond? *J. Am. Chem. Soc.* **2000**, *122* (19), 4750−4755.
(35) Rousseau, G.; Breit, B. Removable Directing Groups in Organic Synthesis and Catalysis. *Angew. Chem., Int. Ed.* **2011**, *50* (11), 2450−2494.

https://dx.doi.org/10.1021/jacs.0c05610
J. Am. Chem. Soc. 2020, 142, 16974−16981